Journal of Hydrology 551 (2017) 423–439

Contents lists available at ScienceDirect

Journal of Hydrology

journal homepage: www.elsevier.com/locate/jhydrol

Research papers

# Development of a hydrological model for simulation of runoff from catchments unbounded by ridge lines

Vamsikrishna Vema [a], K.P. Sudheer [a,b,*], I. Chaubey [b,c]

[a] Department of Civil Engineering, Indian Institute of Technology Madras, Chennai, India
[b] Department of Agricultural and Biological Engineering, Purdue University, West Lafayette, IN, USA
[c] Department of Earth, Atmospheric and Planetary Sciences, Purdue University, West Lafayette, IN, USA

ARTICLE INFO

*Article history:*
Received 25 March 2017
Received in revised form 7 June 2017
Accepted 10 June 2017
Available online 15 June 2017

*Keywords:*
Grid based hydrological model
Administrative catchment
Watershed management

ABSTRACT

Watershed hydrological models are effective tools for simulating the hydrological processes in the watershed. Although there are a plethora of hydrological models, none of them can be directly applied to make water conservation decisions in irregularly bounded areas that do not confirm to topographically defined ridge lines. This study proposes a novel hydrological model that can be directly applied to any catchment, with or without ridge line boundaries. The model is based on the water balance concept, and a linear function concept to approximate the cross-boundary flow from upstream areas to the administrative catchment under consideration. The developed model is tested in 2 watersheds – Riesel Experimental Watershed and a sub-basin of Cedar Creek Watershed in Texas, USA. Hypothetical administrative catchments that did not confirm to the location of ridge lines were considered for verifying the efficacy of the model for hydrologic simulations. The linear function concept used to account the cross boundary flow was based on the hypothesis that the flow coming from outside the boundary to administrative area was proportional to the flow generated in the boundary grid cell. The model performance was satisfactory with an NSE and $r^2$ of $\geq$0.80 and a PBIAS of <25 in all the cases. The simulated hydrographs for the administrative catchments of the watersheds were in good agreement with the observed hydrographs, indicating a satisfactory performance of the model in the administratively bounded areas.



## 1. Introduction

Watershed scale hydrological models are important tools to guide decision making in water resources planning and management. Watershed models represent the hydrological processes and their complex interactions in a simplified manner. These models assist water managers to evaluate the impacts of land/water management practices, climate change etc. on the watershed hydrology (Al Aamery et al., 2016; Arnold et al., 1998; Bergion et al., 2017; Boughton, 2005; Daniel et al., 2011; Guyassa et al., 2017; Miller et al., 2007; Pavelic et al., 2015; Ranatunga et al., 2008; Reddy and Syme, 2015). However, in practice, applications of watershed models in making decisions on water conservation measures or related watershed management (WM) activities have been very few in the developing countries (Reddy and Syme, 2015; Syme et al., 2012). This is plausibly due to the spatial scale on which the WM programs are planned. Generally, the participatory WM programs are planned at a relatively smaller areal extent (ranging from 500 to 5000 ha), not necessarily bounded by ridge lines; rather consider an administrative boundary (at county/village or similar administrative area), which may have trans-boundary flow conditions. Existing watershed models are developed for watersheds defined by topographically derived ridge lines (Arnold et al., 1998; Beven and Kirkby, 1979; Boughton, 2005; Daniel et al., 2011), therefore a direct application of the existing models to these administratively bounded catchments becomes challenging. On the contrary, it can be argued that using a distributed hydrological model (such as SWAT (Arnold et al., 1998), TOPMODEL (Beven and Kirkby, 1979)) can help simulate the processes appropriately in the administrative area of interest by aggregating results from smaller spatial scales of process simulation to larger areas that define the administrative catchment. While this argument is logical, the accuracy of information simulated at different spatial locations by the distributed models depends on the spatial resolution of the available data (land use, soil and topography) (Syme et al., 2012). Fine resolution spatial data for the whole watershed may not be easily available for model

* Corresponding author at: 26, EWRE, Department of Civil Engineering, IIT Madras, Chennai 600036, India.
*E-mail address:* sudheer@iitm.ac.in (K.P. Sudheer).

http://dx.doi.org/10.1016/j.jhydrol.2017.06.012
0022-1694/

setting, but may be available (or can be collected) for small areal extend of interest within the watershed.

The limitations discussed above warrant quantification of water resources and impact assessment of WM practices in the administrative catchments to be done in one of the following ways: (i) by modifying the existing hydrologic model(s), (ii) by using field scale models, or (iii) by developing new hydrological models that can be applied to catchments not necessarily bounded by the ridge lines. Most of the existing hydrological models work on the principle of water balance in a hydrological sub-basin (or response unit), and therefore it is challenging to modify their functionalities to simulate the processes on an administrative catchment with transboundary flow conditions. The second approach is to apply field scale models like EPIC (Sharpley and Williams, 1990), DRIANMOD (Skaggs et al., 2012) etc., to an administrative catchment as a lumped model. This approach tends to ignore the spatial interaction of different mechanisms, and therefore may not be suitable for planning of WM works.

A flexible distributed scheme to represent the attributes such as topography, river network and land use is essential to model the hydrological processes at a finer spatial scale in a catchment (Yang et al., 2000). Depiction of the heterogeneity of catchment landscape and physically based descriptions of hydrological processes has been the focus of the previous studies on distributed hydrological models (e.g. Systeme Hydrologique Europeen (SHE) model – (Abbott et al., 1986); Variable Infiltration Capacity (VIC) model – (Liang et al., 1996); Soil and Water Assessment Tool (SWAT) model – (Arnold et al., 1998)). Spatial scale parameterization of the distributed models has been the consideration by researchers in the recent years (Athira, 2015; Boluwade and Madramootoo, 2013; Yang et al., 2004). Despite these developments, the current hydrological modeling is performed on the full watershed scale. It is pertinent to note that the full watershed span beyond the boundaries of the administrative units. To the best of the knowledge of the authors there are no studies that addressed the hydrological simulations specifically in the administrative unit.

This study proposes a novel hydrological model that can be directly applied to any catchment, with or without traditional ridge line boundaries. The developed model is also based on the water balance concept, but can assess the water resources by simulating the hydrologic processes in the administrative catchment, keeping the spatial interactions intact. The model is developed in MATLAB, and data processing is done using ArcGIS software. This paper introduces the concepts of the administrative catchment hydrological model, and discusses the application of the model in three real-world watersheds.

## 2. Methodology

In the proposed model, a grid-based discretization scheme of watershed is adopted, so as to represent the basin hydrology and transport processes in a spatially distributed approach. Raster datasets are used for land-use, soil, and terrain parameters such as digital elevation model (DEM), flow accumulation, flow direction, and slope gradient. The hydrologic features such as flow accumulation, flow direction and slope are derived from DEM using ArcHydro toolbox in ArcGIS. The D-8 algorithm (O'Callaghan and Mark, 1984) is used to ascertain flow path, and the flow is directed towards the steepest descent among the eight permitted cells. Using the flow direction, grid to grid flow path up to the outlet is obtained. The computational sequence of the model starts from the most upstream cell and moves towards the outlet.

The developed model is based on principle of conservation of mass, and is very similar to that in any general hydrologic model. The model simulates hydrologic cycle based on water balance in each grid using the following equation (Eq. (1)):

$$SW_t = SW_o + \sum_{i=1}^{t}(R_i - Q_i - E_i - Perc_i - gw_i) \quad (1)$$

where $SW_o$ is the initial soil water content at the start of day i and $SW_t$ is the final soil water content, t is time in days, R is precipitation on day i, Q is surface runoff on day i, E is evapotranspiration on day i, Perc is percolation on day i, gw is return flow on day i, i is time step in days; the unit of all variables is mm.

Similar to any watershed model, hydrological processes in this model are simulated using widely accepted and tested methods and algorithms, which are explained in the following sections. The simulation of water balance components like surface runoff, percolation, lateral flow, groundwater flow and evaporation is carried out at every grid cell, and the flow is routed from upstream cells to the outlet. The interaction among the hydrological processes and routing of flow is similar to the schemes used by SWAT (Arnold et al., 1998) and SWATGrid model (Rathjens et al., 2015), thus certain parameters in the proposed model are similar to that of the SWAT model. Fig. 1 shows the conceptual flow of water in the developed model and Fig. 2 shows the computational scheme.

### 2.1. Surface runoff

The model simulates excess rainfall using Soil Conservation Service (SCS) curve number method [USDA-SCS, 1972] for daily rainfall. SCS curve number method accounts for infiltration losses and initial abstraction for computing excess rainfall.

$$Q = \frac{(P - I_a)^2}{P - I_a + S} \quad (2)$$

$$S = \frac{25400}{CN} - -254 \quad (3)$$

where P is precipitation (mm), $I_a$ is initial abstraction (mm), S is potential maximum retention (mm) given by Eq. (3), Q is surface runoff (mm), and CN is SCS curve number, which is a function of a combination of soil, land use, and antecedent soil moisture condition. The soil retention factor S varies with change in soil moisture content, and is updated daily in the model using the following relationship (Arnold et al., 1998):

$$S = S_{max}\left(1 - \frac{SW}{[SW + exp(W_1 - W_2.SW)]}\right) \quad (4)$$

where S is the retention parameter for a given day (mm), $S_{max}$ is the maximum value the retention parameter can achieve (mm), SW is the soil water content of the profile (mm), and $W_1$ and $W_2$ are shape coefficients, determined by solving the above equation based on the assumptions that: (a) the retention parameter for $CN_1$ corresponds to wilting point (AMC I conditions), (b) the retention parameter for $CN_3$ corresponds to the field capacity (AMC II conditions) and (c) the soil has a CN of 99 when completely saturated.

### 2.2. Evaporation and transpiration

Potential evapotranspiration (PET) is estimated by Penman-Monteith equation, using solar radiation, air temperature, relative humidity and wind speed as input data. In the absence of measured data, the solar radiation, relative humidity and wind speed are generated using the WXGEN weather generator model (Arnold et al., 1998; Sharpley and Williams, 1990). The Penman-Moneith Equation for PET (Monteith, 1965) is given by:

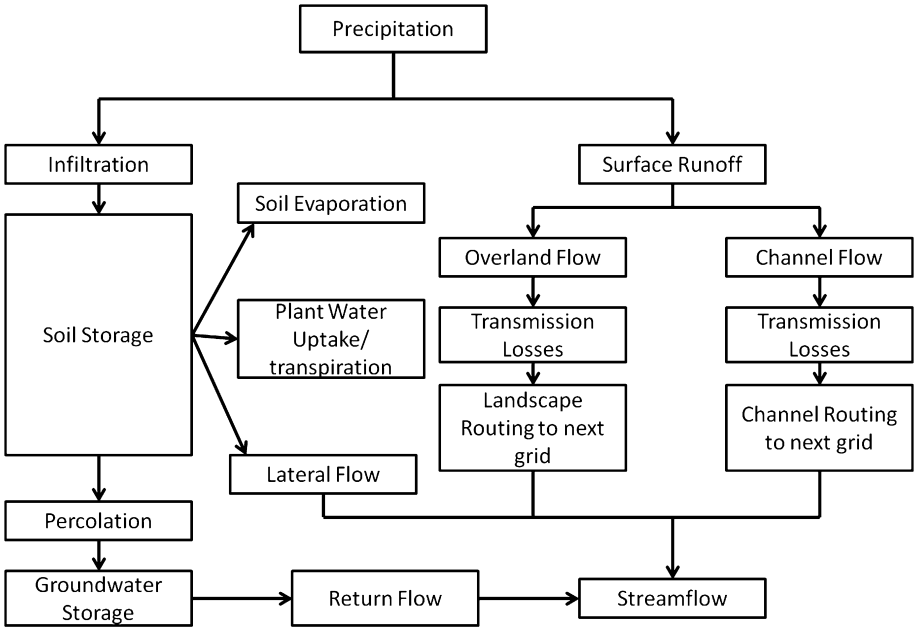


**Fig. 1.** Conceptual framework of the developed model.

$$\lambda ET = \frac{\Delta(R_{net} - G) + \rho_{air}.c_p.\frac{[e_s - e_a]}{r_a}}{\Delta + \gamma.(1 + r_c/r_a)} \quad (5)$$

where λET is latent heat flux density, ET is the depth rate of evapotranspiration, Δ is the slope of saturation vapor pressure – temperature curve, $R_{net}$ is the net radiation, G is the heat flux density to the ground, $\rho_{air}$ is the air density, $c_p$ is the specific heat of air at constant pressure, $e_s$ is saturation vapor pressure, $\gamma$ is the psychrometric constant, $r_c$ is the plant canopy resistance, and $r_a$ is aerodynamic resistance. The PET for a day is divided into maximum transpiration and maximum soil evaporation for the day using an approach similar to Ritchie (1972) and Neitsch et al. (2009). The maximum plant transpiration on a given day is the maximum amount of transpiration from a well-watered plant under neutral atmospheric stability and logarithmic wind profiles (Ritchie, 1972). The soil evaporation is considered to be a fraction of the PET (Ritchie, 1972); the fraction is identified in such a way that the sum of both the maximum transpiration (adjusted to the specific crop condition) and the maximum soil evaporation is equal to the PET. Since both transpiration and soil evaporation are to be met from the available soil moisture in different soil layers, the following procedure is employed in this model.

The actual soil evaporation is calculated by partitioning the maximum soil evaporative demand between the different layers of the soil profile. The following distribution (Eq. (6)) is used to determine the maximum evaporative demand from each soil layer along the depth (Neitsch et al., 2009):

$$E_z = E_s\left(\frac{z}{z + \exp(2.374 - 0.00713.z)}\right) \quad (6)$$

where $E_z$ is the evaporative demand at depth z (mm), $E_s$ is the maximum soil water evaporation (mm) and z is the depth below the soil surface. The coefficients of the equation are such that 50% of the demand is extracted from top 10 mm and 95% from the top 100 mm of the soil profile.

The evaporative demand for the soil layer is determined by taking the difference between the evaporative demands of the upper and lower boundaries of the layer, by appropriately accounting for the soil moisture redistribution along the depth:

$$E_{ly} = E_{zl} - E_{zu}.esco \quad (7)$$

where $E_{ly}$ is the evaporative demand for the layer (mm), $E_{zl}$ is the evaporative demand at the lower boundary of the soil layer (mm), $E_{zu}$ is the evaporative demand at the upper boundary of the soil layer and esco is soil evaporation compensation coefficient to modify the depth distribution of the soil evaporative demand. The range of esco is 0.1–1.0; a lower value of esco corresponds to higher extraction of soil water from lower layers of soil profile, while a higher value corresponds to higher extraction from top of the layer. The evaporative demand for the soil layer is adjusted if the water content of the soil layer is below the field capacity (Neitsch et al., 2009).

The plant water uptake, which caters to the transpiration demand, is modeled in a similar approach as that of soil evaporation. The potential plant water uptake from the soil surface to any depth in the root zone is estimated using the following distribution (Neitsch et al., 2009):

$$W_{up} = \frac{E_t}{[1 - \exp(-\beta_w)]}\left[1 - \exp\left(-\beta_w.\frac{z}{z_{root}}\right)\right] \quad (8)$$

where $W_{up}$ is the potential plant water uptake from the soil surface to a specified depth, Z, on a given day (mm), $E_t$ is the maximum plant transpiration on a given day (mm), $\beta_w$ is the water-use distribution parameter, z is the depth from the soil surface (mm), and $z_{root}$ is the depth of root in the soil (mm). The potential water uptake from each soil layer in the root zone is computed by taking the difference between the plant water uptake demands of upper and lower boundaries of the layer using an expression similar to Eq. (7). The plant water uptake is adjusted if the moisture content of the soil layer is less than the field capacity of the soil layer (Neitsch et al., 2009). When the soil moisture available in the upper layers of the soil profile are unable to meet the full plant water uptake demand for that layer, the remaining demand for those layers is extracted from the lower layers of the soil profile.

### 2.3. Infiltration

The water remaining after evapotranspiration and runoff, infiltrates into the soil layer. The model assumes that the infiltrated

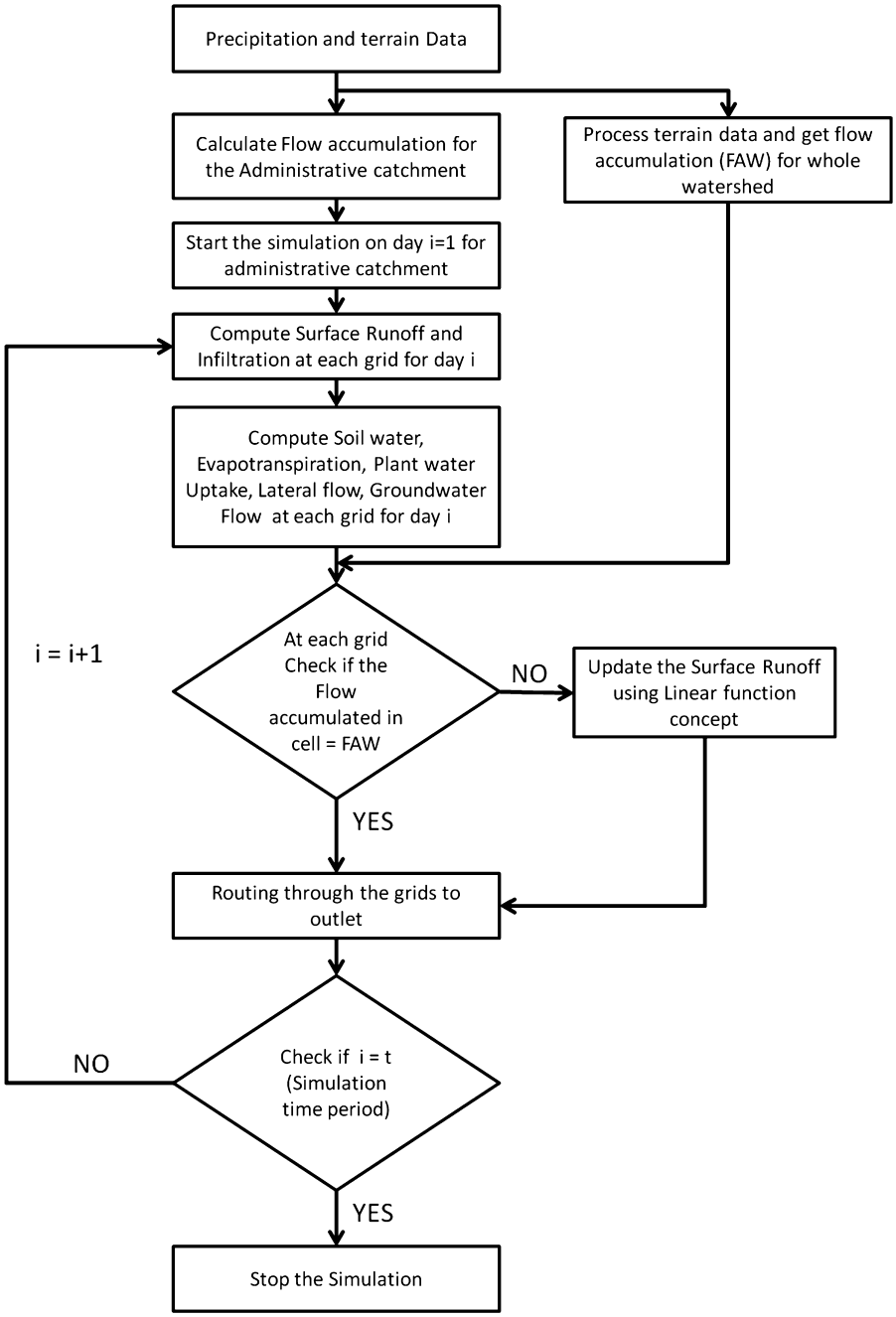


**Fig. 2.** Computational scheme of the developed model.

water is instantaneously distributed uniformly in the layer. The water percolates to the next layer only if the moisture content exceeds the field capacity of the soil layer. The water percolating out of the last layer is added to the aquifer recharge. The percolation for each soil layer is calculated by:

$$Perc_{ly} = SW_{excess,ly}\left(1 - \exp\left(\frac{-\Delta t}{TT}\right)\right) \quad (9)$$

where $Perc_{ly}$ is the amount percolating to the next layer (mm), $SW_{excess,ly}$ is amount of soil water in excess of the field capacity in the soil layer, $\Delta t$ is the length of the time step (h), and TT is the travel time for percolation (h). The travel time for percolation is calculated for each layer using:

$$TT = \frac{SAT_{ly} - FC_{ly}}{K_{sat}} \quad (10)$$

where $SAT_{ly}$ is the saturation soil water (mm), $K_{sat}$ is the saturated hydraulic conductivity for the layer (mm/h), and $FC_{ly}$ is field capacity of the soil layer (mm). The field capacity of the soil layer is estimated by:

$$FC_{ly} = WP_{ly} + AWC_{ly} \quad (11)$$

where $WP_{ly}$ is the wilting point of the soil layer and $AWC_{ly}$ is the available water capacity of the soil layer to be given as input to the model, and needs to be calibrated.

### 2.4. Lateral flow

Lateral flow volume is computed with a kinematic storage model (Sloan and Moore, 1984) as a function of slope, slope length, porosity and saturated hydraulic conductivity.

$$Q_{lat} = 0.024.\left(\frac{2.SW.K_{sat}.s}{\varphi_d.sl}\right) \quad (12)$$

where $Q_{lat}$ is lateral flow volume (mm), SW is soil water (mm), $K_{sat}$ is saturated hydraulic conductivity (mm/h), s is slope (m/m), sl is slope length (m) and $\varphi_d$ is the porosity. Lateral flow accumulated over the soil profile flows to the adjacent downstream grid and gets distributed in the soil layers.

### 2.5. Groundwater flow

Groundwater flow is simulated in the model by creating an aquifer below the soil profile using the linear tank storage model (Arnold et al., 1993; Neitsch et al., 2009; Sangrey et al., 1984). The flow percolating out of the last soil layer is assumed as groundwater recharge. The groundwater contributes to the stream flow only when the depth of water in aquifer is above a threshold depth (gwqmn). The amount of groundwater contributing the stream flow is computed by:

$$Q_{gw,i} = Q_{gw,i-1}.exp[-\alpha_{gw}.t] + Perc_{rchrg,i}(1 - exp[-\alpha_{gw}.\Delta t]) \quad (13)$$

$$Perc_{rchrg,i} = \left(1 - exp\left[\frac{-1}{\partial_{gw}}\right]\right).Perc_l + exp\left[\frac{-1}{\partial_{gw}}\right].Perc_{rchrg,i-1} \quad (14)$$

where $Q_{gw,i}$ is the groundwater flow into the main channel on day i (mm), $Q_{gw,i-1}$ is the groundwater flow into the main channel on day i−1 (mm), $\alpha_{gw}$ is the base flow recession constant, $\Delta t$ is the time step. $Perc_{rchrg,i}$ is the amount of recharge entering the shallow aquifer on day i (mm), $Perc_{rchrg,i-1}$ is the amount of recharge entering the shallow aquifer on day i−1 (mm), $Perc_l$ is the amount of water percolating from last layer of the soil profile to the aquifer, and $\partial_{gw}$ is the delay time of the geologic formation.

### 2.6. Overland and channel flow in the grids

Each grid will have run-on from upstream grids, and runoff generated within the grid. The runoff generated within the grid is assumed to be available at the grid outlet. Incoming runoff to each grid is partitioned into two components, overland and channel flow, using the concept of hydrological sensitive areas proposed by Rathjens et al. (2015). The upstream grids, where channels are getting generated, will have dominant landscape flow, and the downstream grids, where the channels are well developed, will have dominance of channel flow compared to overland flow. Lyon et al. (2004) suggested that Topographic Index (TI), can be used to identify high runoff potential areas, which are dominated by channel flow. The TI is defined as (Lyon et al., 2004):

$$\lambda = \ln\left(\frac{A_i}{\tan(B_i).K_i.Z_i}\right) \quad i = 1,\ldots,n;\ \forall A_i > 0 \quad (15)$$

where λ is the topographic index, $A_i$ is the upslope contributing area per unit contour length ($m^2/m$), $B_i$ is the local topographic slope angle (radian), $K_i$ is the saturated hydraulic conductivity (m/day), and $Z_i$ is the soil depth (m). The λ takes a value which is non-zero and positive. The spatial variability of λ indicates the spatial variability of runoff potential of grids; higher value of λ indicating larger runoff potential. The value of λ will be high for grids in the downstream areas of the watershed, compared to upstream grids; the order of increase of λ (spatial direction) will be in line with the natural drainage path. The λ is scaled to vary between zero and one using the computed minimum and maximum value of λ within the watershed, and is used as a factor to divide the generated runoff into channel (factor equal to λ) and overland flow (factor equal to 1−λ) components in every grid.

Location of the channel head initiation is an important information for realistically representing the flow process in the watershed. Traditionally, channel delineation using DEM is achieved by providing a contributing area as threshold for channel head formation. Whereas, in the case of TI, the channel head initiation is performed by considering an analogy between the drainage network and the TI network. The flow length in each grid is weighted by the TI, normalized by the drainage area, and the sum of the weighted flow length for all the grids is equivalent to the drainage density. Therefore the following equation is considered.

$$DD \approx \frac{\sum_{i=1}^{n} \lambda_i^n l_i}{DA} \quad (16)$$

where DD is the drainage density of the watershed, $\lambda_i^n$ is the scaled TI, $l_i$ is the contour length per unit cell length, and DA is the total drainage area of the watershed. The value of TI for grids with smallest value of TI are re-set to zero iteratively until the equation (16) become valid. After the re-set, the grids with a smallest value will act as the channel head. A similar procedure was employed by Rathjens et al. (2015) in the development of SWATgrid model.

The two components, overland flow and channel flow, are routed in the grid, and are considered joining together with the runoff generated within the grid at the outlet of the grid. The overland flow (partitioned from the incoming runoff) in each grid is routed to its outlet using the procedure outlined by Rathjens et al. (2015). This approach employs the overland flow velocity and travel time for each grid, which are computed using Manning's equation (Arnold et al., 2010). The partitioned channel flow in each grid is routed towards the outlet of the grid using the variable storage routing method (Williams, 1969) that is employed in many hydrological models (Arnold et al., 1995; Williams and Haan, 1973). The grid to grid routing is executed by considering a linear system of reservoirs (Nash, 1957). In this method, each grid is considered to be one reservoir, and the water flows from one grid to subsequent grid along the direction of flow. The transmission and storage losses are appropriately considered before the water moves from one reservoir to the next, and were appropriately accounted in the water balance for the grid.

### 2.7. Inflow at the administrative boundary of the catchment

Unlike the regular ridge line bounded watersheds, the administrative catchments can receive water across its boundary. Therefore, this inflow to the administrative catchments from upstream areas are to be accounted while simulating the hydrological processes in the administrate catchment. This study envisaged the following procedure to account the cross-boundary inflow, considering the fact that the administrative catchment is a part of a much larger master watershed that is bounded by ridge lines. For instance, the Fig. 3(a) is a topographic sketch map of a hypothetical master watershed and Fig. 3(b) is a topographic sketch map of an administrative catchment within this hypothetical master watershed, each depicting the DEM of the area. The flow direction, and subsequently the flow accumulation in each grid can be estimated using the DEM. The D-8 algorithm (O'Callaghan and Mark, 1984) is considered in this study for flow accumulation, and is done independently for the master watershed (Fig. 3(c)) and the administrative catchment (Fig. 3(d)). It is clear from the Fig. 3(c) and (d) that the flow accumulation at some of the boundary grids of the administrative catchment is different from the flow accumulation on the same grids in the master watershed. The difference in the flow accumulation in corresponding grids, at the

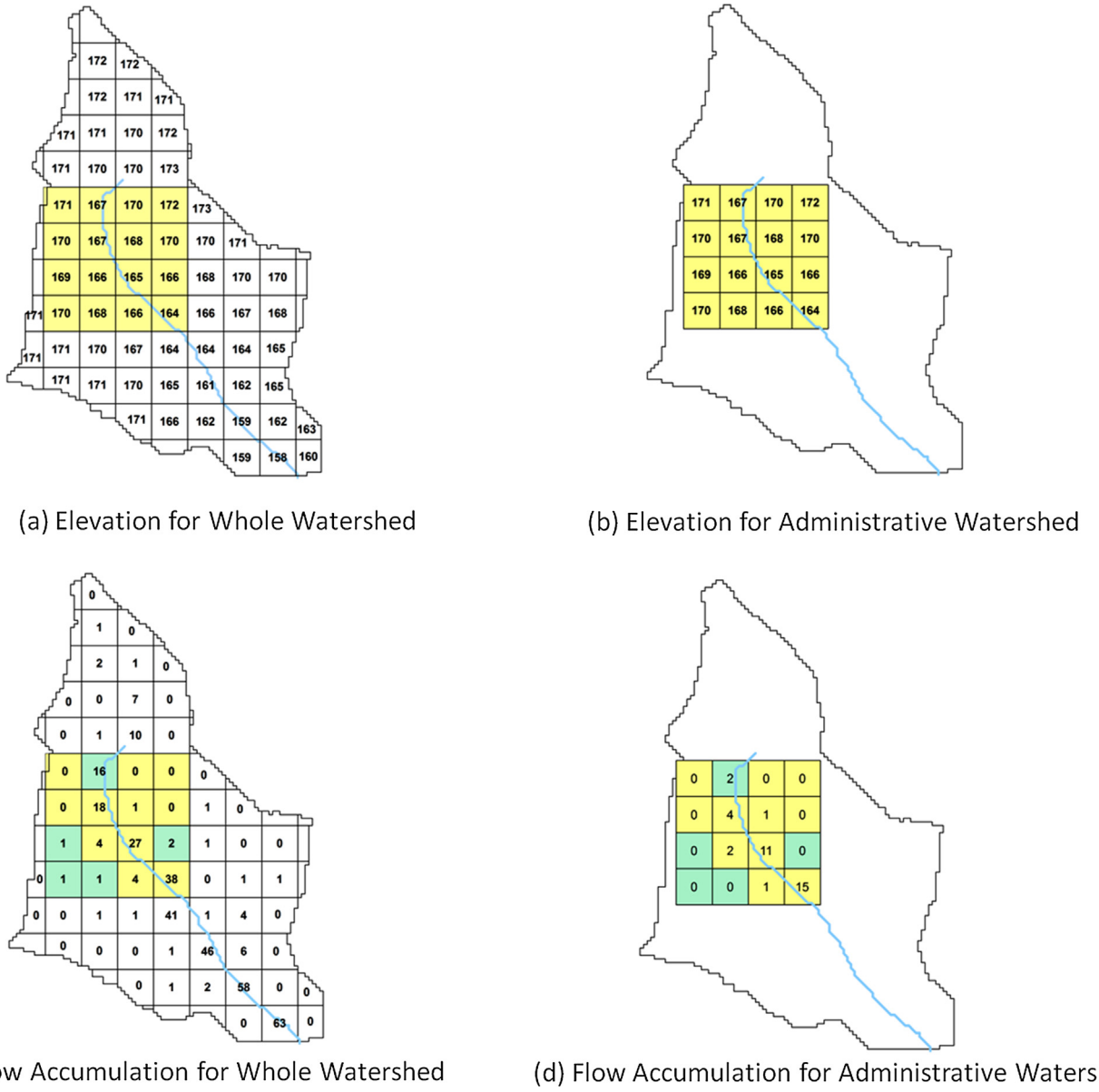


**Fig. 3.** Example sketch to demonstrate the estimation of inflow to the boundary grids of the administrative catchments (The yellow shaded cells in the watershed are the hypothetical administrative area and the Blue shaded cells in (c) and (d) are boundary cells. The second cell in the first row in (d) has 2 grids draining into it, while in the whole watershed in (c) same grid has 16 grids draining into it. Therefore the flow form remaining 14 grids is estimated using the developed relationship as f = Q * 14 * W). (For interpretation of the references to colour in this figure legend, the reader is referred to the web version of this article.)

boundary of administrative catchment, indicates the number of grids draining from upstream of boundary grids to the respective grids. Note that this can be true for all the boundary grids in the administrative catchment. Therefore, the flow from these upstream grids needs to be appropriately accounted in the simulation.

The routing of flow from grid to grid is in the form of a series of cascading reservoirs (Nash, 1957), which is a linear system as mentioned earlier. Therefore, in this approach, the flow from upstream areas (consisting of a group of grids) to any grid in the downstream will be proportional to the number of contributing grids. Consequently, it is hypothesized that the amount of flow coming from the upstream grids to the administrative catchment (cross-boundary flow) is proportional to the number of upstream contributing grids at that boundary grid. Based on this hypothesis, it is proposed that the incoming flow at the boundary cell can be estimated as a product of runoff (generated at the boundary grid), and the number of upstream contributing grids (outside the boundary of the administrative catchment). In order to consider the variability of soil and land use characteristics of the grids, the proposed inflow to the boundary grid of the administrative catchment is adjusted by introducing a parameter, W, in the proposed relationship. Accordingly, the inflow to the boundary grids is computed using the following equation:

$$f_i = Q_i \times FA \times W \tag{17}$$

where $f_i$ is incoming flow to the $i^{th}$ boundary grid, $Q_i$ is runoff generated in the $i^{th}$ boundary grid, $\Delta FA$ is difference in flow accumulated at the grid considering the master watershed and the administrative watershed, and W is a parameter, which accounts for upstream catchment characteristics and is an input parameter. The validity of the proposed relationship is verified in the case examples presented in this paper, and is discussed in the later sections.

The value of 'W' will depend on the characteristics of the upstream grids in terms of runoff generation. The value of 'W' will be low, if the upstream contributing grids are low runoff generating as compared to the boundary grids, and will be high in the case of high runoff generating grids on the upstream. The value is found to be less than 1.0, for upstream grids with relatively less runoff generation characteristics as compared to boundary grids. On the other hand, if the upstream grids produce relatively higher runoff as compared to boundary grids, the value of 'W' is found to be >1.0, and goes up to 3.0 (based on the numerical exercises done in this study). Ideally, the value of 'W' needs to be estimated through calibration of the model. In the absence of observed flow data for calibration, an appropriate value of 'W' is to be chosen by considering the drainage characteristics, the soil and the land use, which indicate the runoff potential, of the upstream of boundary grids as compared to full watershed.

## 3. Case examples: study watersheds and data

The proposed model is envisaged to be used for simulating hydrological processes in areas not bounded by ridge lines to aid in developing WM plans. Accordingly, two case examples are presented to evaluate the effectiveness of the model simulations in small watersheds as well as relatively larger watersheds. First Case Example (CE-A) is for two watersheds in the consortium of watersheds at Riesel, Texas, USA, which is an experimental watershed maintained by the USDA. The second example (CE-B) is on a subwatershed of the Cedar creek watershed, Texas, USA, which is a part of the Upper Trinity River basin. The criteria for selection of the watersheds for this study was that the watershed should be small with first or second order stream network as the WM in the developing countries is mostly practiced in headwater or lower order streams especially for water conservation.

### 3.1. Case example (A)

The experimental watersheds in the Riesel, Texas, were established in 1937 by the USDA–ARS Grassland Soil and Water Research Laboratory. This experimental station, which is a part of the Brushy Creek watershed, consists of 10 small watersheds, where most of the hydrological and meteorological parameters are measured continuously. For this Case Example (A), two watersheds with gauge stations W1 and Y2 were considered (Fig. 4). The catchment area of these two stations are 70.4 ha and 53.4 ha, respectively. Land use in these watersheds consists predominantly of pasture, rangeland, and agricultural areas with rotation of corn, wheat and sorghum. Climate is characterized by long hot summers and short mild winters, with an annual average precipitation of 890 mm. Both watersheds are dominated by Houston Black clay soils. The soil is well drained and slow permeable with an average saturated hydraulic conductivity of 0.765 mm/h. The Houston Black soil has a typical texture of 17% sand, 28% silt, and 55% clay, and is widely recognized as classical vertisol (Arnold et al., 2010; Steiner et al., 2009). Runoff and climate datasets were provided by the USDA's research station.

The hydrological model was setup for the two watersheds for 9 years (1995–2003), with 3 initial years as warm up period. The average annual rainfall during the model run period in W1 and Y2 watersheds was 886 mm and 887 mm, respectively. The average runoff during the same period is 111 mm and 136 mm for W1 and Y2 watersheds respectively with negligible base flow.

Initially, the proposed model was setup for the entire hydrologic watershed boundary of W1 and Y2 (Fig. 4(a) and (c)), and the observed data was used for evaluating the model conceptualization and structure. Later, two pseudo administrative catchments in W1 and Y2 watersheds were assumed, and the model was further tested. To validate the simulations of the proposed model using observed records, the pseudo-administrative watersheds were considered draining to the outlets of the hydrologic watershed as shown in Fig. 4(b) and (d).

### 3.2. Case example (B)

A 48 km$^2$ sub-watershed of Cedar Creek in Van Zandt county of Texas (Fig. 4(e) and (f)) is used to demonstrate the effectiveness of the proposed model in a relatively larger watershed. The watershed is located entirely in the Cedar creek watershed, which is a part of upper Trinity River basin. Topographic elevation of the study area range from 171 m to 123 m above mean sea level. Climate of the selected sub-watershed is classified as subtropical-humid climate with an average rainfall of 990.6 mm. The amount of rainfall varies considerably from year to year, with spring being the typical wettest season. Soils within the watershed are loamy at the surface and clayey at the subsurface, and major land use in the watershed is pasture covering about 85% of the area. Similar to case example (A), a pseudo administrative boundary was setup such that the outlet of the pseudo administrative boundary matched with sub-basin outlet (Fig. 4(e) and (f)). Observed record of stream flow was not available for verification, as there was no gauge station at the outlet of the sub watershed. Therefore, the effectiveness of the simulation by the proposed model was tested by comparing it against simulated output from the SWAT model, which has been applied on this basin by various researchers (Cibin et al., 2014; Narasimhan et al., 2010) for multiple studies in the past.

The proposed model is setup from 1964 to 1970 to simulate the hydrology of the administrative catchment. The SWAT model was also setup for the total watershed for the same period. Fig. 4 (e) and (f) show the subbasin and the selected administrative catchment. Digital elevation model, land use map, soil map and climatic data were obtained from the USGS.

## 4. Performance evaluation of the simulations

The model simulations were evaluated using three statistical performance measures: Nash Stutcliffe Efficiency (NSE) (Nash and Sutcliffe, 1970), coefficient of determination ($r^2$) and Percent Bias (PBIAS). Range of NSE is from $-\infty$ to 1, where 1 represents perfect model and 0 represents that the model is no better than taking the mean of observed time series at all time steps (Dawson et al., 2007). The $r^2$ is an index similar to NSE, but indicates variance in the measured data explained by the linear model. PBIAS measure the tendency of the simulated output to over predict or under predict than the observed data. Positive values of PBIAS indicate model underestimation while negative values indicate model overestimation (Moriasi et al., 2007). These indices are defined as follows:

$$NSE = 1 - \frac{\sum_{i=1}^{n}(Y_{oi} - Y_{si})^2}{\sum_{i=1}^{n}(Y_{oi} - \overline{Y_{oi}})^2} \tag{18}$$

$$PBIAS = \left[\frac{\sum_{i=1}^{n}(Y_{oi} - Y_{si})}{\sum_{i=1}^{n} Y_{oi}}\right] \times 100 \tag{19}$$

$$r^2 = \left[\frac{\sum_{i=1}^{n}(Y_{oi} - \overline{Y_{oi}})(Y_{si} - \overline{Y_{si}})}{\sqrt{n\sum Y_{oi}^2 - (\sum Y_{oi})^2}\sqrt{n\sum Y_{si}^2 - (\sum Y_{si})^2}}\right]^2 \tag{20}$$

where $Y_{oi}$ is observed data at i$^{th}$ time step, $Y_{si}$ is simulated output at i$^{th}$ time step and $\overline{Y}_{oi}$ is the mean of the observed data and $\overline{Y}_{si}$ is the mean of the simulated data.

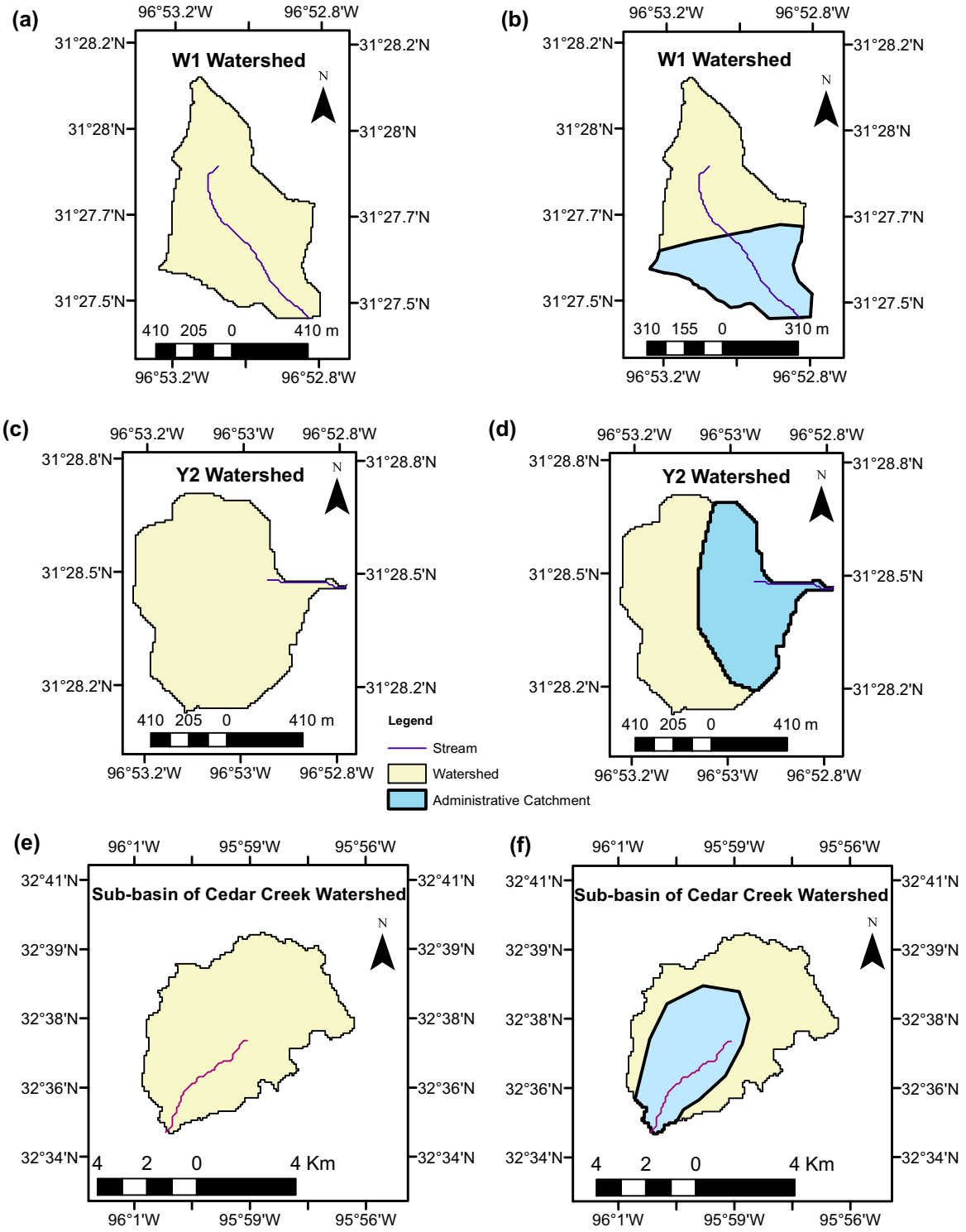


**Fig. 4.** Sketch of full and administrative watersheds considered in this study: (a) Riesel W1 full watershed, (b) Riesel W1 administrative watershed, (c) Riesel Y2 full watershed, (d) Riesel Y2 administrative watershed, (e) Subbasin of Cedar Creek watershed, and (f) Administrative catchment in the subbasin of the Cedar Creek watershed.

## 5. Results and discussions

### 5.1. Case example (CE-A)

As discussed earlier, the proposed model is applied to the full watershed (independently to W1 and Y2) to evaluate the effectiveness of the conceptual framework of the model. The simulated and measured hydrograph is presented Fig. 5, for both W1 and Y2 watersheds. The results indicate that the model appropriately responds to the rainfall events, and the stream flow simulations are satisfactory (Fig. 5(b)) for both watersheds. The flow events in both low and high flow conditions are well captured by the model, and the trends of the observed hydrograph is simulated well by the model, as can be evidenced from high $r^2$ value of 0.78 and 0.81 for W1 and Y2 watersheds respectively. Note that the hydrograph in Fig. 5 is for an uncalibrated model. The model,

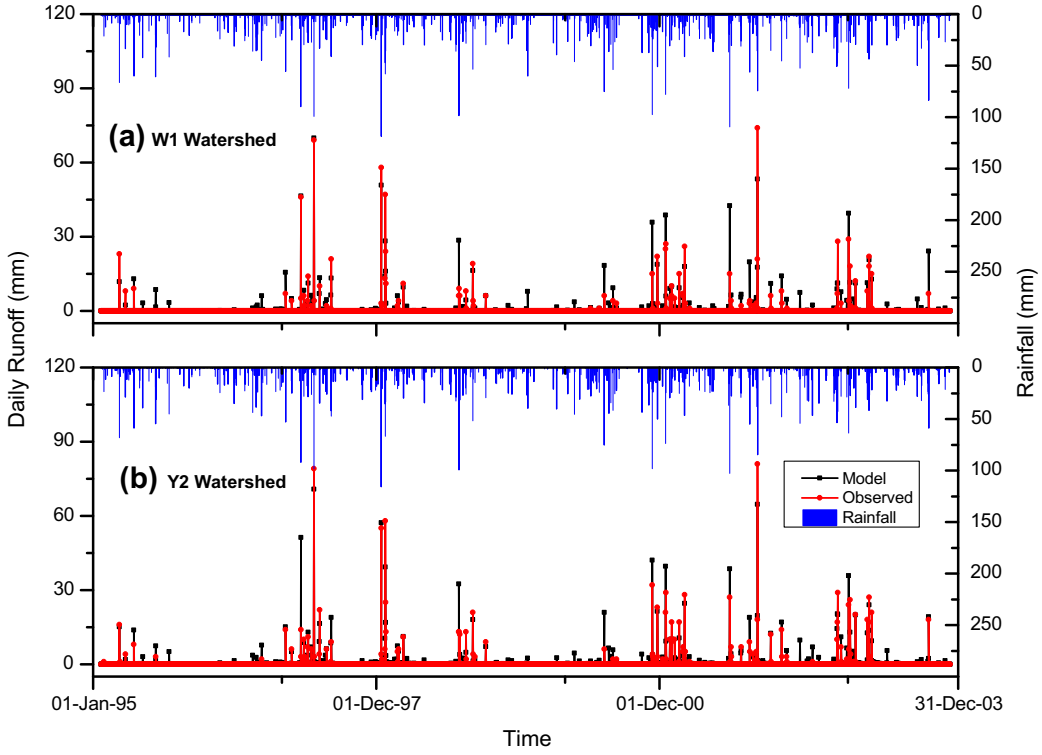


**Fig. 5.** Uncalibrated model results for (a) W1 watershed and (b) Y2 watershed.

however, tends to under-predict the discharge peaks in the initial period and over predict in the later periods of the simulation. Also, the low flow periods are over-predicted with some of the no-flow conditions simulated with positive flows. To address these limitations, model was subject to calibration subsequently.

Fig. 6 shows the spatial variation of land use, soil, average annual actual evapotranspiration, average annual runoff, and average annual soil water in the W1 watershed. It is noted from Fig. 6 that the spatial variability of the simulated hydrological components are in line with the spatial heterogeneity present in the watershed in terms of land use and soil. As expected, the actual evapotranspiration and runoff is high from agricultural areas and rangeland. Also it can be observed that actual evaporation is more dependent on the soil characteristics, while runoff generation is more inclined towards the land use.

*5.1.1. CE-A: calibration and validation of the model*

The calibration of the model was performed by considering a split sample validation approach. The first 3 years of simulation period (from 1998 to 2003) was considered as warm up period, the next 4 years (1998–2001) was considered as the calibration period. The balance period of 2 years (2002–2003) was considered for validation of the model. The model has 6 parameters to be estimated, and additional parameter would arise when the model is applied to an administrative watershed. The description of parameters and the potential range of values is presented in Table 1. All the parameters were calibrated by using the objective function of maximizing NSE for both the watersheds, and the calibrated values of the parameters are presented in Table 1. Note that the value parameter w, reported in Table 1 is not applicable to the full watershed (the value is for the administrative watershed).

Precipitation in the Riesel watershed is highly variable from year to year as well as within any given year, with long term annual average of 890 mm (Steiner et al., 2009). During the period of simulation excluding the warm-up period (1995–1997), precipitation varied between 500 mm and 1284 mm, with an average of 899 mm. In most years, rainfall amount is low with occasional long periods of no rainfall. Similar to the variation in rainfall, the observed annual runoff varies from 6 mm to 217 mm in W1 watershed while in Y2 watershed it varies from 9 mm to 282 mm. It is to be noted that the maximum flow was observed in the year 2001, while the maximum precipitation was in 2000. This could be attributed to the long spells of drought in the years 1998 and 1999. This behavior was captured by the model effectively.

The daily runoff hydrograph for the calibration period for W1 (Fig. 7(a)) and scatter plot of simulated vs. observed runoff events of Y2 (Fig. 8) watersheds indicate that the developed model simulate the flow hydrograph satisfactorily. The flow simulation of low flow regions and zero flow conditions is satisfactory with reduction of flow events during zero flow conditions compared to the uncalibrated model result. Also the flow events are captured well by the model, as can be seen from the scatter plot (Fig. 8) of the simulated vs. observed runoff events for the Y2 watersheds. It is to be noted that the peak runoff in W1 is over estimated by the model, whereas the peak runoff in Y2 is underestimated. This may be plausibly due to less effectiveness in the simulation of sub-surface flow (which affects the saturation level of the soil and the delay in reaching to the groundwater) by the model, as there is a reversal in the error between the initial and final time periods of the simulation. However, the error in simulation is not significant (less than 25% PBIAS in both the watersheds), which is considered to be a satisfactory performance (Moriasi et al., 2007).

Statistical performance measures for the model simulations in full watershed are presented in Table 2. The values indicate good model performance in both calibration and validation periods with NSE greater than 0.8 in both the cases. Monthly performance measures are better than the daily values, a result which can be visualized by the monthly flow hydrographs in Fig. 9 and Fig. 10 for W1 and Y2 watershed respectively and is often observed in hydrological model applications (Moriasi et al., 2007; Rathjens et al., 2015).

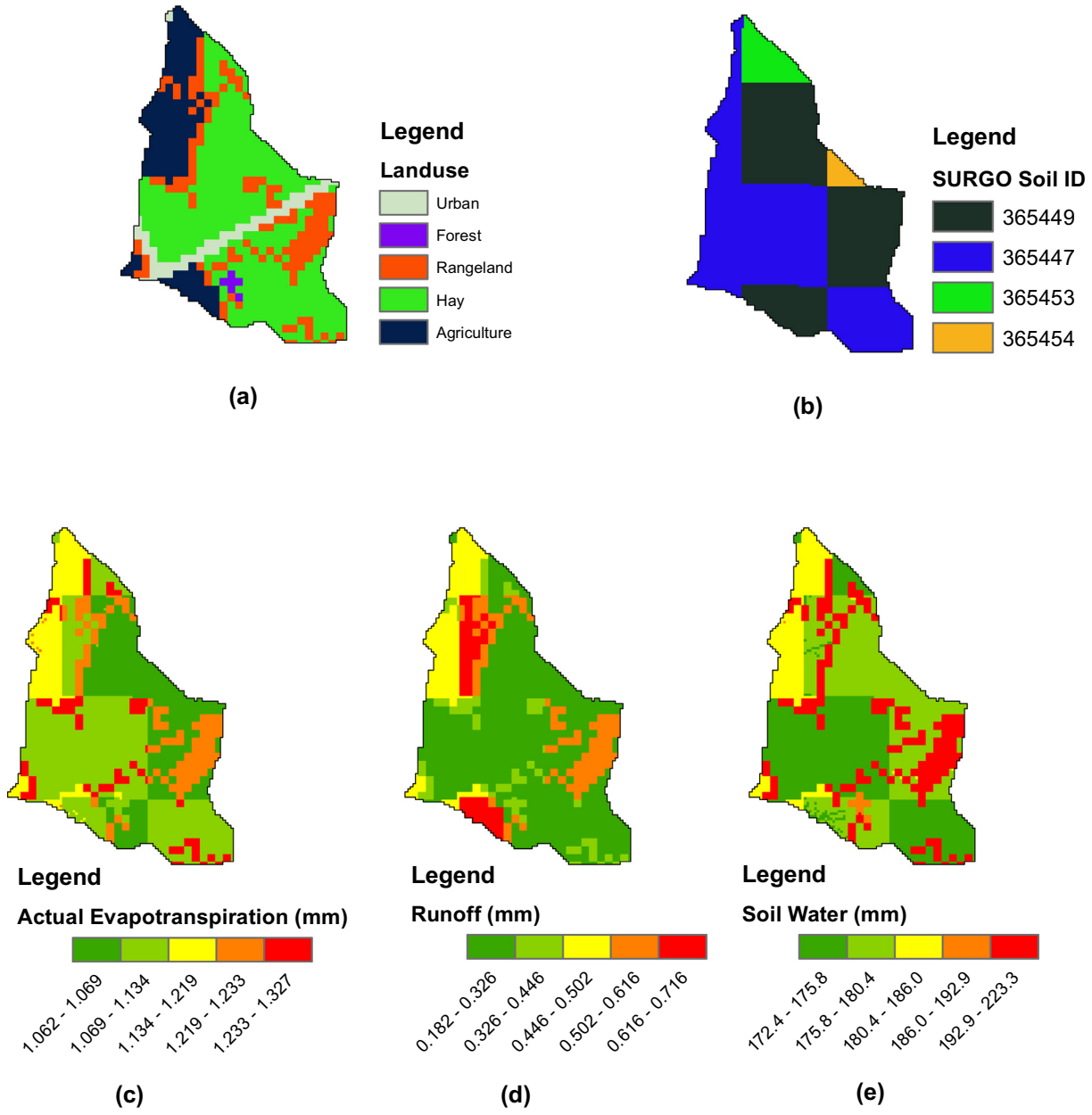


**Fig. 6.** Spatial distribution of (a) Landuse, (b) Soil, (c) Annual average actual evapotranspiration, (d) estimated runoff, and (e) Soil water of W1 watershed in Riesel.

**Table 1**
Calibration parameters of the model.

| Model Parameter | Description | Units | Range | Calibrated parameters | | | |
|---|---|---|---|---|---|---|---|
| | | | | W1 Full | W1 Admin | Y1 Full | Y1 Admin |
| CN | Curve Number | % | ±0.5 | −0.17 | −0.18 | −0.21 | −0.11 |
| AWC | Initial soil available water content | % | ±0.3 | 0.034 | 0.062 | 0.3 | 0.064 |
| ESCO | Soil compensation factor, which divides the evaporation demand between soil layers | – | 0.1–1 | 0.92 | 1 | 1 | 0.94 |
| gwqmn | Aquifer depth above which base flow starts | mm | 0–3000 | 734.1 | 191.8 | 148.7 | 264.9 |
| Alphabf | Base flow recession constant | – | 0–1 | 0.1 | 0.66 | 0.11 | 0.16 |
| gwdelay | Delay factor for the base flow | – | 0–1 | 0.1 | 0.48 | 0.1 | 0.37 |
| W | Factor for accumulating the upstream flow contribution to the boundary grids | – | – | – | 0.23 | – | 0.11 |

*5.1.2. Validation of the linear function hypothesis*

As the primary objective of this study is to develop a model for simulating the hydrology in an administrative catchment, the proposed model has been tested for two administrative catchments in the W1 and Y2 catchments. During the conceptual development of the proposed administrative watershed model, a linear function

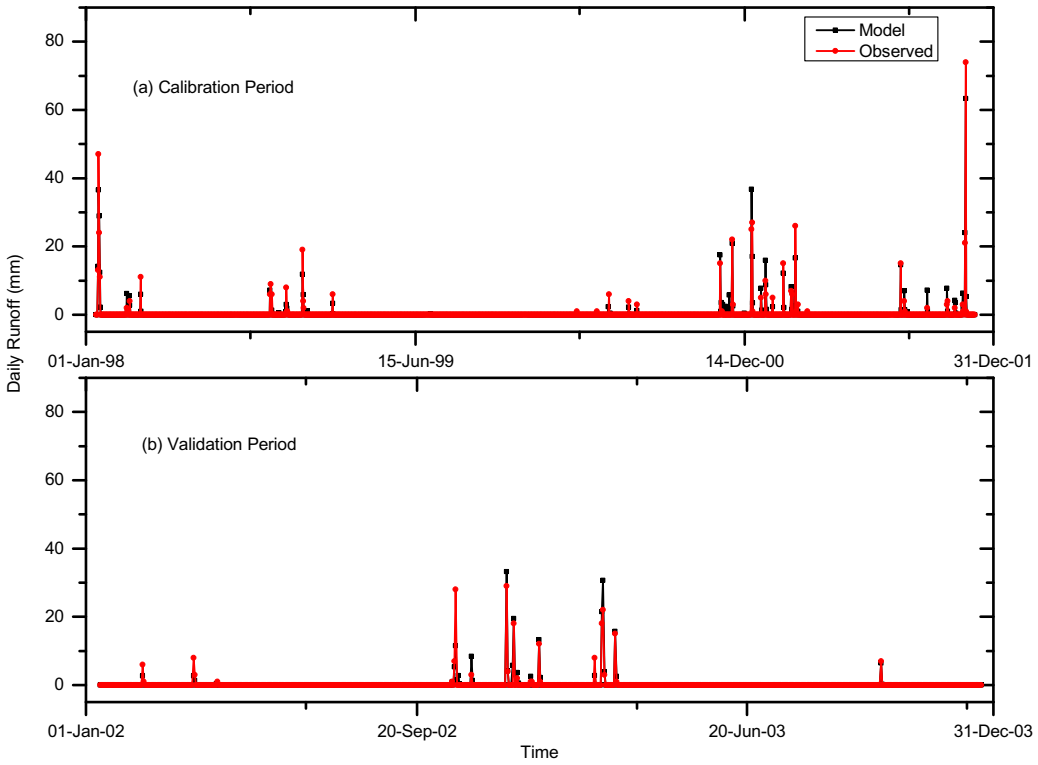


**Fig. 7.** Simulated hydrograph (daily) of W1 watershed for: (a) calibration period and (b) validation period.

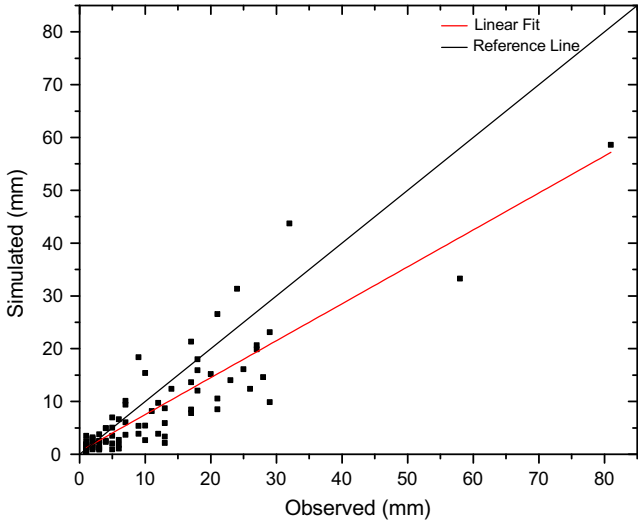


**Fig. 8.** Scatter plot of simulated vs. observed for runoff events for Y2 watershed.

was assumed (discussed in Section 2.7) between the flow incoming to the boundary cells and flow generated in the boundary cells. For example, W1 administrative watershed, the upstream area drained into 36 boundary cells. In order to validate the efficacy of the linear function concept, the flow at the administrative boundary cells, incoming and generated, were extracted from the full watershed model, and analyzed. The results for 4 such boundary cells (cells 1, 4, 15 and 24) shown in Fig. 11 are presented in Fig. 12. A linear relationship between the incoming and generated flows at the cells is evident from the scatter plots (Fig. 12). The results clearly illustrate the validity of the conceptual framework of the model.

### 5.1.3. Performance of the model in administrative catchment

The proposed models was applied to the two administrative watersheds in W1 and Y2, and calibrated/validated using the data pertaining to 1995–2003. The model was calibrated for all 7 parameters using the objective function of maximizing NSE. The statistical performance indices NSE and $r^2$ are presented in Table 3. It is evident from the Table 3 that the proposed model is effectively simulating the hydrological processes in the administrative watershed. As anticipated, the monthly scale performance measures are better compared to the daily scale measures. The simulations in the administrative catchment in terms of the indices are similar to that in the full catchment by the model, which indicated a reasonably good estimation of the inflow to the boundary cells. Comparison of simulated and observed daily runoff hydrographs of the W1 watershed indicates that the developed model satisfactorily

**Table 2**
Summary of the statistical parameters for the whole watersheds of WI and Y2.

| | Watershed | NSE | | $r^2$ | | PBIAS (%) |
|---|---|---|---|---|---|---|
| | | Daily | Monthly | Daily | Monthly | |
| Calibration | W1 | 0.91 | 0.95 | 0.91 | 0.96 | −4.24 |
| | Y2 | 0.82 | 0.86 | 0.85 | 0.89 | 18.65 |
| Validation | W1 | 0.84 | 0.9 | 0.85 | 0.95 | −5.29 |
| | Y2 | 0.87 | 0.94 | 0.87 | 0.94 | 3.24 |

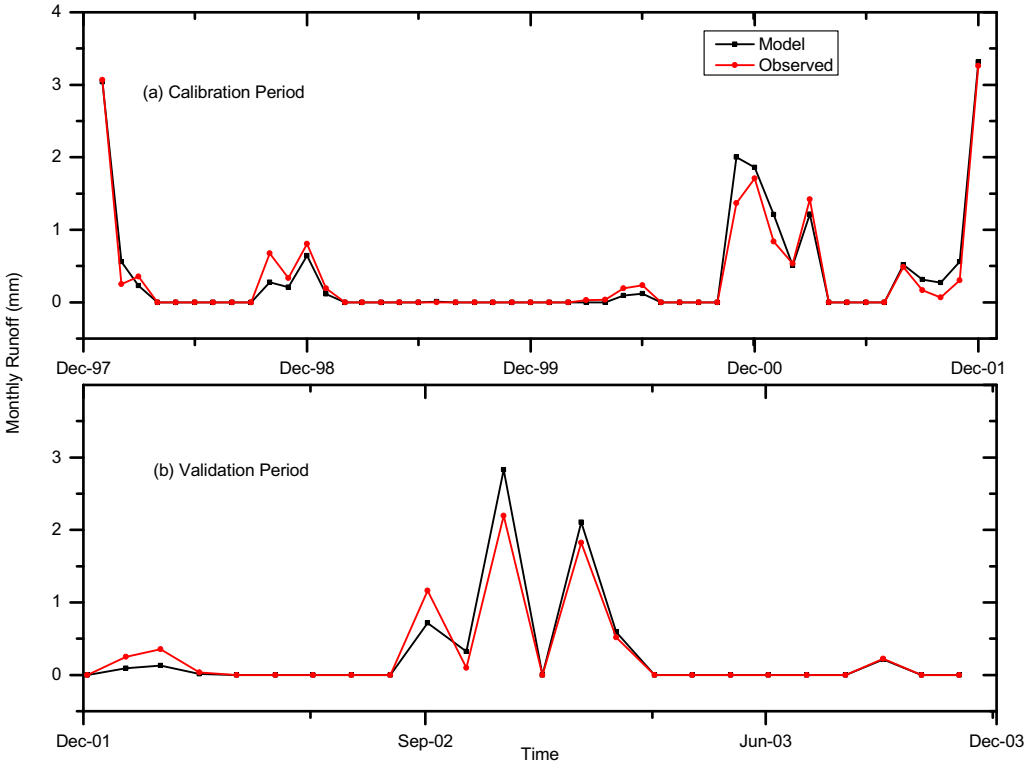


**Fig. 9.** Simulated hydrograph (monthly) for W1 watershed: (a) calibration period, (b) validation period.

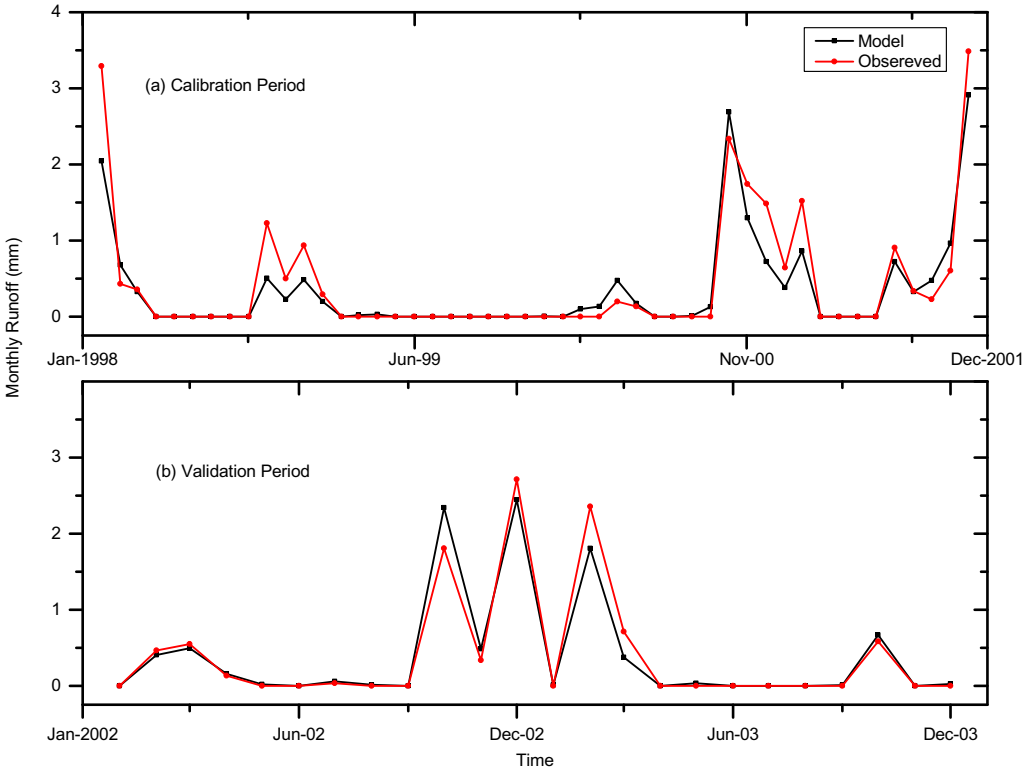


**Fig. 10.** Simulated hydrograph (monthly) for Y2 watershed: (a) calibration period, (b) validation period.

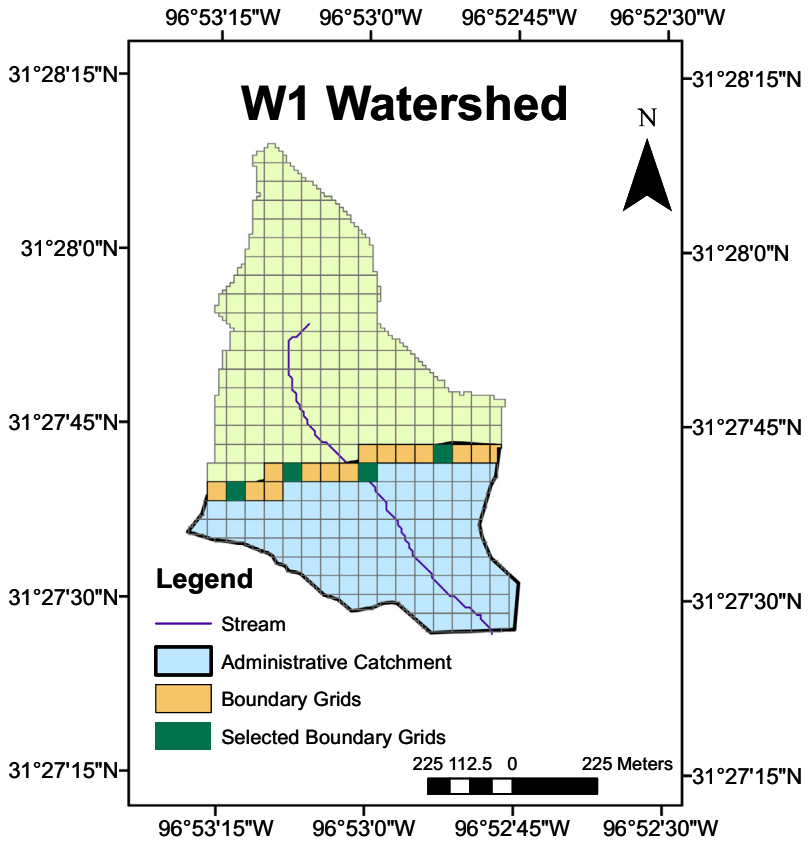


**Fig. 11.** Riesel W1 watershed showing boundary grids (The grids shown in figure are at coarser resolution (50 × 50 m) than the data considered for simulation (10 × 10 m)).

simulates the hydrological processes in the administrative catchments. In this case also, there is a bias in the simulation of peak events (in both W1 and Y2), however were within acceptable limits (PBIAS < 25%). The simulated hydrograph for Y2 watershed show good correlation with the observed flows, and it can be noted that low flow events are mostly under predicted for both the watersheds. Similar results can be seen from the monthly hydrographs (Fig. 13), with the model under predicting in the Y2 watershed and over predicting in some months in the W1 watershed.

*5.1.4. Estimation of parameter 'W'*

The model's efficacy depends on the value chosen for 'W' in the Eq. (17). As mentioned earlier, the 'W' is a parameter that signifies the runoff characteristics of the upstream contributing area (upstream of the administrative boundary), and moderate the incoming runoff to the administrative catchment in the model. The physiographic factors that affect the runoff, in general, include drainage area, slope, roughness, storage, drainage density, channel length and antecedent moisture conditions of the contributing area (Tarboton, 2003). Ideally, 'W' is to be calibrated along with other parameters of the model, as is done in the case examples in this study. However, in cases, where measured stream flow is not available for calibration, the value of 'W' has to be appropriately chosen. Typically 'W' can be considered as a function of drainage density, CN and main channel length of the upstream contributing area in comparison with that of the full watershed. The runoff is considered to be varying directly with the second power of the drainage density (Carlston, 1963). The drainage area ratio has been used to approximate the flow at an ungauged location in a watershed (USEPA, 2007). Therefore, an appropriate value of the 'W', can be obtained by conditioning (product) the square of the drainage density of the upstream contributing area on the ratio of drainage area, CN and channel length of the contributing area to that of the full watershed. In the case of Y2 watershed, the drainage density of the upstream contributing area was 0.98 km/km$^2$. The drainage density, when conditioned on the fraction (ratio) of the contributing area (0.56) and the channel length ratio (0.30), along with the ratio of the CN (upstream area and full watershed) resulted in a value of 0.16. Accordingly, an initial value of 0.16 was considered for 'W' during calibration. The calibrated value of 'W' for Y2 was 0.11. In a similar way, for the watershed W1, drainage density (1.32 km/km$^2$), fraction of contributing area (0.57), and channel length ratio (0.42) and CN ratio (1.0) suggested a value of 0.44 to 'W', as compared to the calibrated value of 0.33. Note that one may need to perform a sensitivity analysis to finalize the appropriate value. Any available information on the stream flow will be handy at this stage. It may be noted that this calculation procedure, though logical, needs reinforcement with the help of simulations in a large number of watersheds.

*5.2. Case example B (CE-B)*

In addition to the simulation of two pseudo administrative catchments in the Riesel watershed, an administrative catchment (pseudo) in the subbasin of Cedar Creek watershed is also simulated. This simulation exercise was to evaluate the model performance in a larger basin. As mentioned earlier, in the absence of observed records, SWAT model output was used to evaluate the proposed model's performance. Cedar creek is a well managed watershed in terms of nutrient delivery and erosion control, and many researchers have successfully used SWAT model to simulate the hydrology and water quality in the Cedar creek (Cibin et al.,

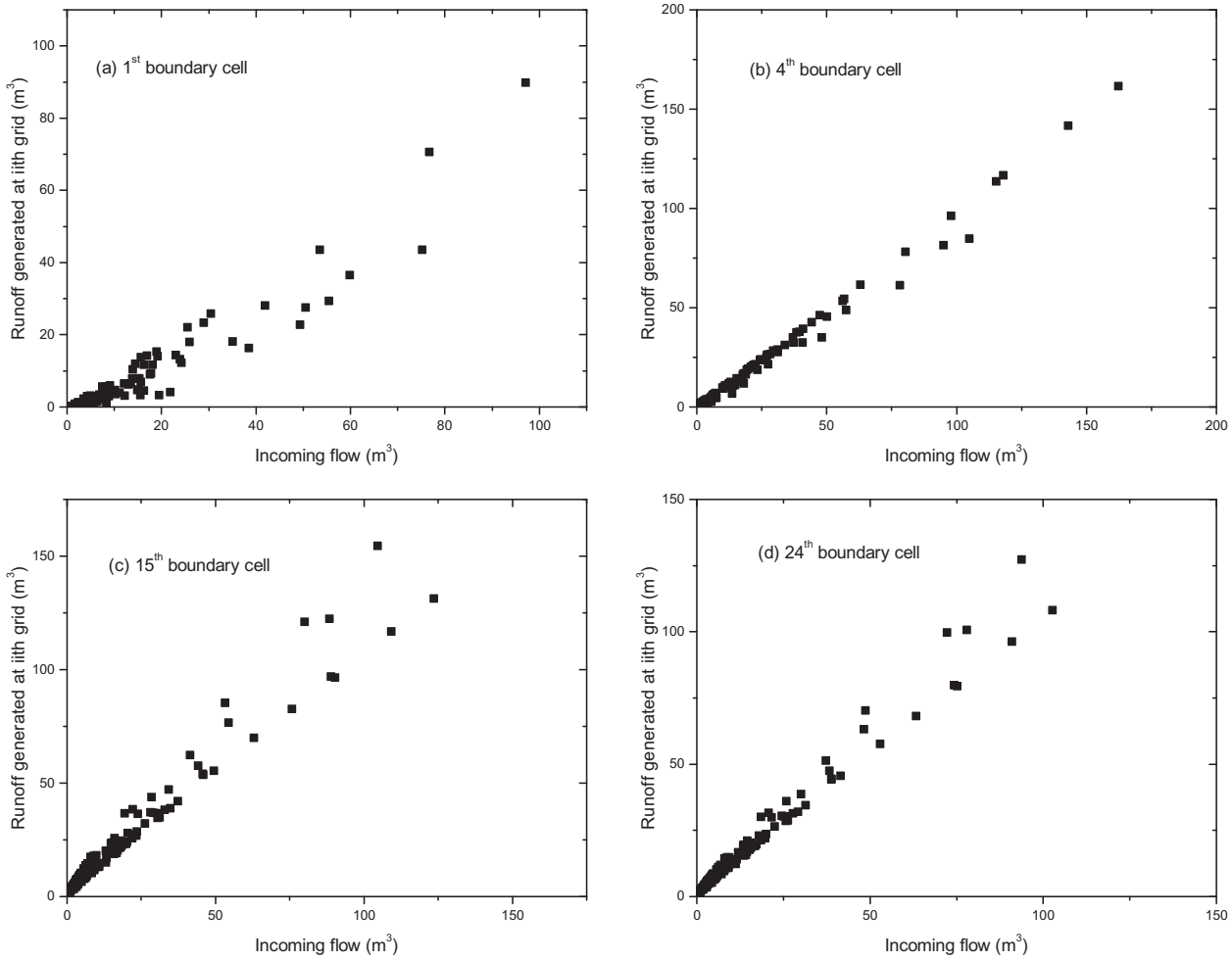


**Fig. 12.** Scatter plot comparing runoff generated in $i^{th}$ boundary against incoming flow from upstream areas.

**Table 3**
Summary of calibration and validation results for administrative watersheds.

| | Watershed | NSE | | $r^2$ | | PBIAS (%) |
|---|---|---|---|---|---|---|
| | | Daily | Monthly | Daily | Monthly | |
| Calibration | W1 | 0.81 | 0.88 | 0.82 | 0.89 | −11.43 |
| | Y2 | 0.87 | 0.92 | 0.89 | 0.95 | 23.66 |
| Validation | W1 | 0.80 | 0.97 | 0.82 | 0.97 | −8.07 |
| | Y2 | 0.81 | 0.91 | 0.85 | 0.96 | 25.66 |

2014; Narasimhan et al., 2010). One of the main requirement for SWAT model to effectively simulate the nutrient delivery and soil erosion is that the model should simulate the stream flow effectively. Therefore, stream flow generated by the SWAT model (calibrated and validated) can be considered for a comparison with the stream flow from proposed model.

The area of simulation is much larger in this example (48 $km^2$) compared to that of CE-A (0.70 $km^2$). Therefore, the upstream contributing area to the administrative catchment is also relatively large. All of the upstream areas drained to the administrative boundary at 74 boundary cells. The number of upstream contributing cells in these 74 boundary cells ranged from 1 to 1342. The runoff contribution to and generated at selected boundary cells are presented in Fig. 14, to evaluate the linear function relationship conceptualized in the model. The cells considered were 2, 5, 19 and 44 receiving flow from 6, 228, 59 and 1342 upstream cells respectively. The scatter plots (Fig. 14) of the selected 4 boundary cells confirms the linear relationship between incoming and generated flows in the cells, thus validating the assumed relationship for larger watersheds and higher number of the contributing cells.

The performance of the developed model in simulating the flow hydrograph is very much similar to the SWAT model as can be seen from Fig. 15(a). All the peaks and low flows are well captured by the proposed model for the administrative catchment, which is important for the planning of appropriate WM measures. Comparison of monthly flow hydrographs (Fig. 15(b)) indicates that the hydrological processes are satisfactorily simulated by the proposed model. This observation is endorsed by the statistical performance measures of the daily and monthly simulations of the developed model – NSE of 0.90 and 0.91 for daily and monthly simulations respectively.

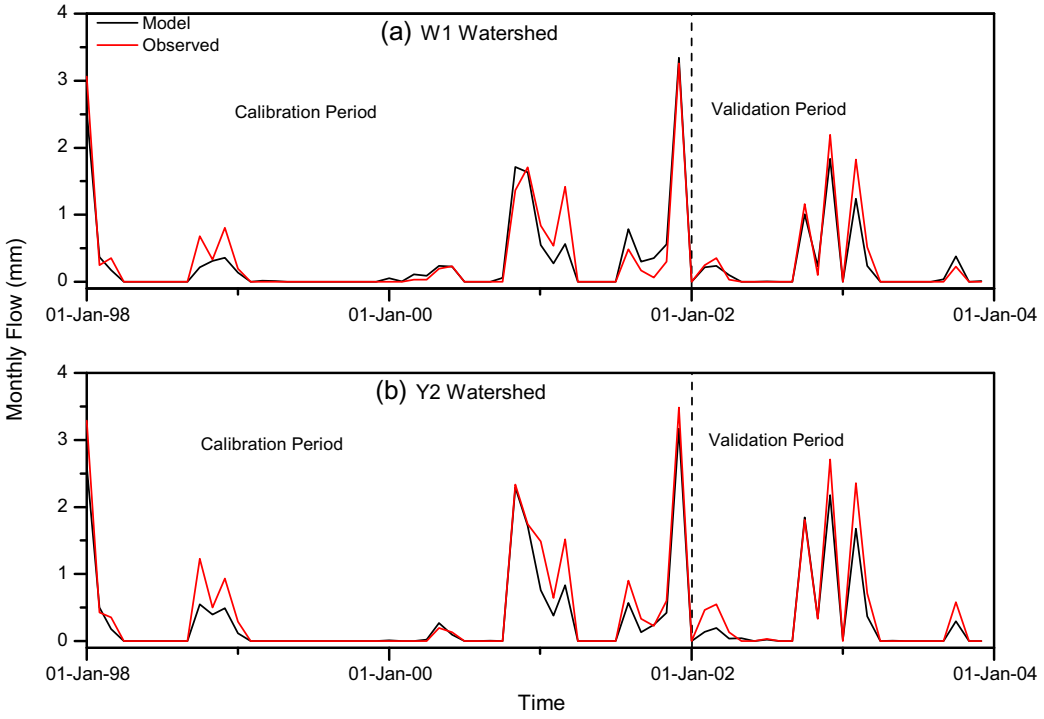


**Fig. 13.** Simulated and observed monthly hydrographs for (a) W1 watershed and (b) Y2 watershed.

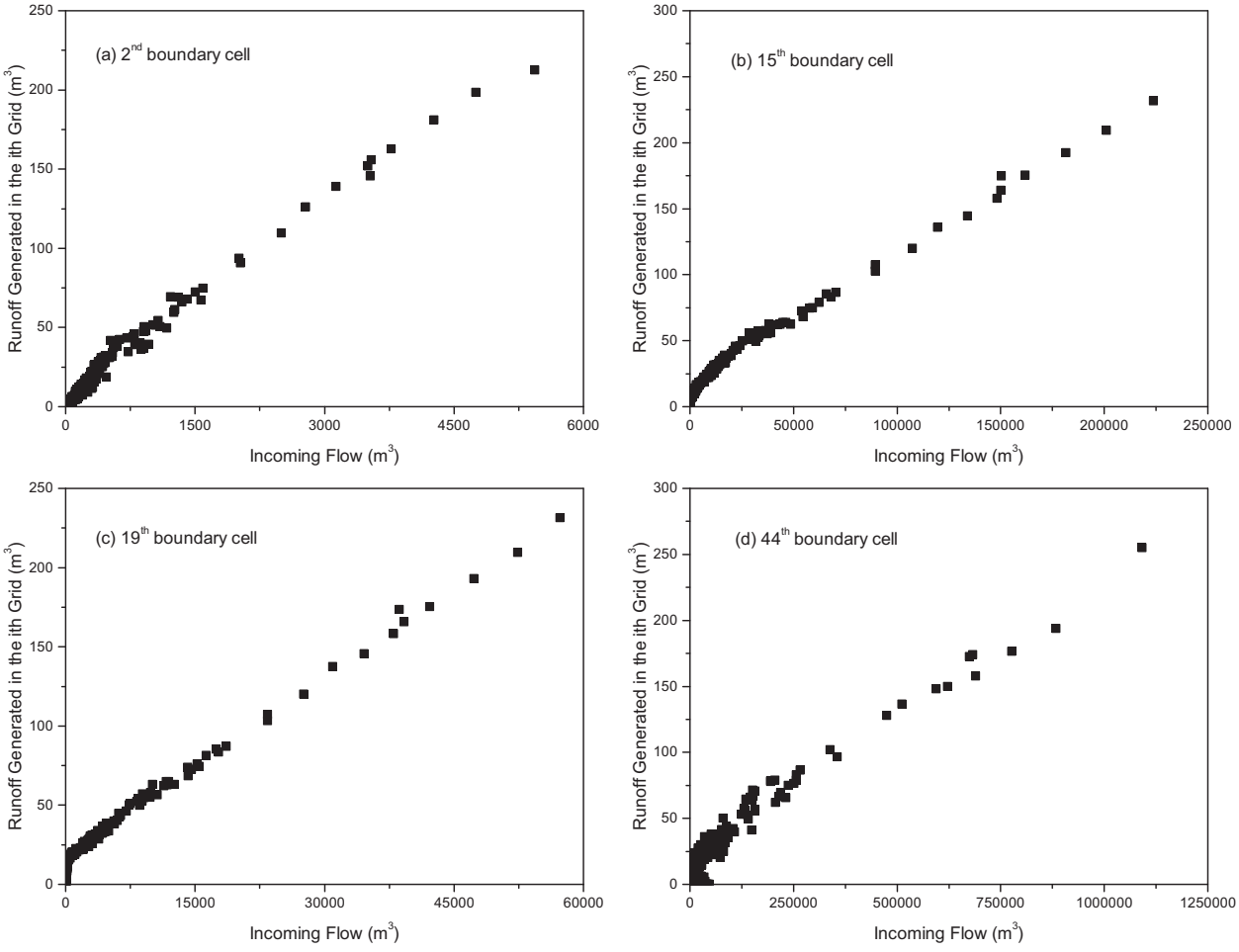


**Fig. 14.** Scatter plot comparing runoff generated in $i^{th}$ boundary cell against incoming flow from upstream areas for Sub-basin of Cedar Creek Watershed.

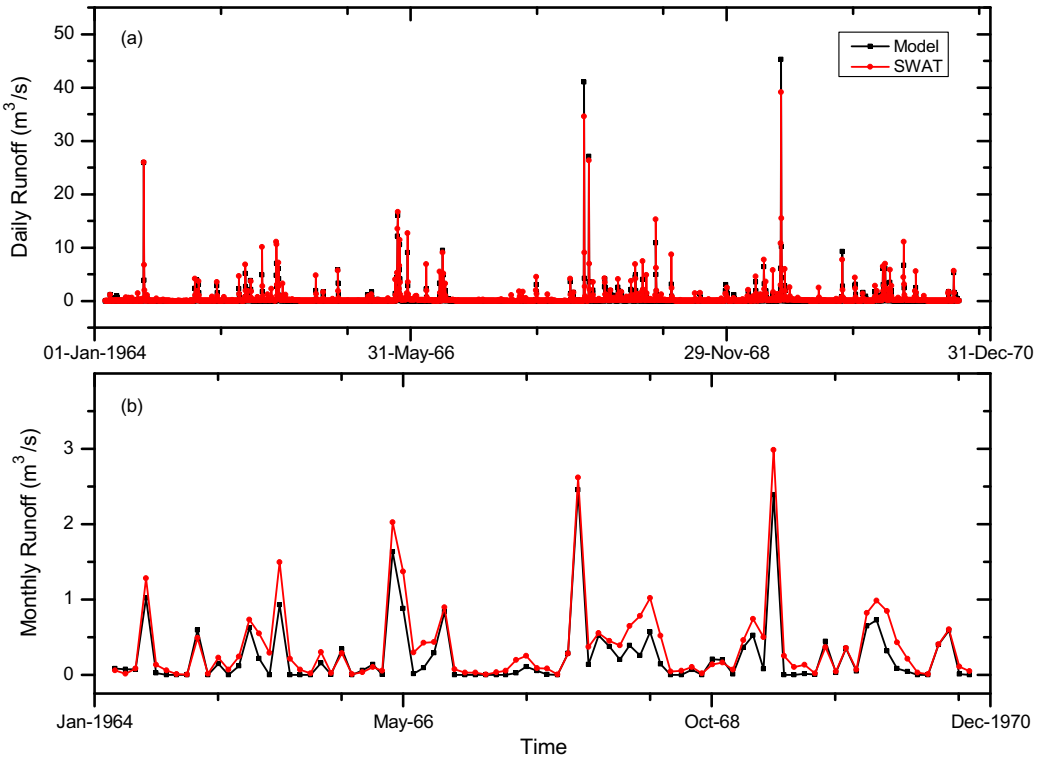


**Fig. 15.** Simulated hydrograph for developed model and SWAT (a) Daily Flow, (b) Monthly Flow.

## 6. Conclusive remarks

The conceptual development and application of a grid based hydrological model for administrative catchments is presented in this study. The requirement of simulation in administrative catchments mainly stem from the need for developing WM practices in areas that are not bounded by regular ridge lines. Since the currently available hydrological models cannot be directly applied for such simulations, the model proposed in this study is a good initiative in that direction. The success of such models majorly depend on how effectively one is able to factor the upstream runoff contributions to the administrative catchments through its boundary. The upstream contribution to the boundary of the administrative catchment was conceptualized as linear function of the runoff generated at the boundary, and this was shown to be effective through the example case studies. It is also demonstrated that the proposed model satisfactorily simulates the hydrology of the full watershed, as well as that of the pseudo administrative watersheds. The simulated hydrograph had only a little deviation from observed hydrograph for the full watershed simulation of both W1 and Y2 catchments in Riesel.

## References


Abbott, M.B., Bathurst, J.C., Cunge, J.A., O'Connell, P.E., Rasmussen, J., 1986. An introduction to the European hydrological system-systeme hyrdrologique Europeen, "SHE", 2: structure of a physically-based, distributed modelling system. J. Hydrol. 87, 61–77. http://dx.doi.org/10.1016/0022-1694(86)90115-0.

Al Aamery, N., Fox, J.F., Snyder, M., 2016. Evaluation of climate modeling factors impacting the variance of streamflow. J. Hydrol. 542, 125–142. http://dx.doi.org/10.1016/j.jhydrol.2016.08.054.

Arnold, J.G., Allen, P.M., Bernhardt, G., 1993. A comprehensive surface-groundwater flow model. J. Hydrol. 142, 47–69. http://dx.doi.org/10.1016/0022-1694(93)90004-S.

Arnold, J.G., Allen, P.M., Volk, M., Williams, J.R., Bosch, D.D., 2010. Assessment of different representations of spatial variability on SWAT model performance. Trans. ASABE 53, 1433–1443.

Arnold, J.G., Srinivasan, R., Muttiah, R.S., Williams, J.R., 1998. Large area hydrologic modeling and assessment Part I: model development. J. Am. Water Resour. Assoc. 34, 73–89.

Arnold, J.G., Williams, J.R., Maidment, D.R., 1995. Continuous-time water and sediment-routing model for large basins. J. Hydraul. Eng. 121, 171–183. http://dx.doi.org/10.1061/(ASCE)0733-9429(1995) 121:2(171).

Athira, P., 2015. Regionalization of Hydrological Models: A Method to Predict Streamflow in Ungauged Basins and to Quantify the Predictive Uncertainty. Indian Institute of Technology Madras, Chennai.

Bergion, V., Sokolova, E., Astrom, J., Lindhe, A., Soren, K., Rosen, L., 2017. Hydrological modelling in a drinking water catchment area as a means of evaluating pathogen risk reduction. J. Hydrol. 544, 74–85. http://dx.doi.org/10.1016/j.jhydrol.2016.11.011.

Beven, K.J., Kirkby, M.J., 1979. A physically based, variable contributing area model of basin hydrology/Un modèle à base physique de zone d'appel variable de l'hydrologie du bassin versant. Hydrol. Sci. Bull. 24, 43–69. http://dx.doi.org/10.1080/02626667909491834.

Boluwade, A., Madramootoo, C., 2013. Modeling the impacts of spatial heterogeneity in the castor watershed on runoff, sediment, and phosphorus loss using SWAT: I. Impacts of spatial variability of soil properties. Water Air Soil Pollut., 224, 1692. doi: 10.1007/s11270-013-1692-0.

Boughton, W., 2005. Catchment water balance modelling in Australia 1960–2004. Agric. Water Manag. 71, 91–116. http://dx.doi.org/10.1016/j.agwat.2004.10.012.

Carlston, C.W., 1963. Drainage density and streamflow. U.S. Geol. Surv. Prof. Pap. No. 42 2–C, 8pp.

Cibin, R., Athira, P., Sudheer, K.P., Chaubey, I., 2014. Application of distributed hydrological models for predictions in ungauged basins: a method to quantify predictive uncertainty. Hydrol. Process. 28, 2033–2045. http://dx.doi.org/10.1002/hyp.9721.

Daniel, E.B., Camp, J.V., Leboeuf, E.J., Penrod, J.R., Dobbins, J.P., Abkowitz, M.D., 2011. Watershed modeling and its applications: a state-of-the-art review. Open Hydrol. J. 5, 26–50.

Dawson, C.W., Abrahart, R.J., See, L.M., 2007. HydroTest: a web-based toolbox of evaluation metrics for the standardised assessment of hydrological forecasts. Environ. Model. Softw. 22, 1034–1052. http://dx.doi.org/10.1016/j.envsoft.2006.06.008.

Guyassa, E., Frankl, A., Zenebe, A., Poesen, J., Nyssen, J., 2017. Effects of check dams on runoff characteristics along gully reaches, the case of Northern Ethiopia. J. Hydrol. 545, 299–309. http://dx.doi.org/10.1016/j.jhydrol.2016.12.019.

Liang, X., Lettenmaier, D.P., Wood, E.F., 1996. One-dimensional statistical dynamic representation of subgrid spatial variability of precipitation in the two-layer variable infiltration capacity model. J. Geophys. Res. Atmos. 101, 21403–21422. http://dx.doi.org/10.1029/96JD01448.

Lyon, S.W., Walter, M.T., Steenhuis, T.S., 2004. Using a topographic index to distribute variable source area runoff predicted with the SCS curve-number equation. Hydrol. Process. 18, 2757–2771. http://dx.doi.org/10.1002/hyp.1494.

Miller, S.N., Semmens, D.J., Goodrich, D.C., Hernandez, M., Miller, R.C., Kepner, W.G., Guertin, D.P., 2007. The automated geospatial watershed assessment tool. Environ. Model. Softw. 22, 365–377. http://dx.doi.org/10.1016/j.envsoft.2005.12.004.

Monteith, J.L., 1965. Evaporation and environment. Symp. Soc. Exp. Biol. 19, 205–224.

Moriasi, D.N., Arnold, J.G., Liew, M.W..Van., Bingner, R.L., Harmel, R.D., Veith, T.L., 2007. Model evaluation guidelines for systematic quantification of accuracy in watershed simulations. Trans. ASABE 50, 885–900.

Narasimhan, B., Srinivasan, R., Bednarz, S.T., Ernst, M.R., Allen, P.M., 2010. A comprehensive modeling approach for reservoir water quality assessment and management due to point and nonpoint source pollution. Trans. ASABE 53, 1605–1617. http://dx.doi.org/10.13031/2013.34908.

Nash, J.E., 1957. The Form of the Instantaneous Unit Hydrograph. IAHS Publ..

Nash, J.E., Sutcliffe, J.V., 1970. River flow forecasting through conceptual models part I—a discussion of principles. J. Hydrol. 10, 282–290. http://dx.doi.org/10.1016/0022-1694(70)90255-6.

Neitsch, S., Arnold, J.G., Kiniry, J.R., Williams, J.R., 2009. Soil & Water Assessment Tool Theoretical Documentation Version 2009.

O'Callaghan, J.F., Mark, D.M., 1984. The extraction of drainage networks from digital elevation data. Comput. Vision, Graph. Image Process. 28, 323–344. http://dx.doi.org/10.1016/S0734-189X(84)80011-0.

Pavelic, P., Xie, J., Sreedevi, P.D., Ahmed, S., Bernet, D., 2015. Application of a simple integrated surface water and groundwater model to assess mesoscale watershed development. In: Reddy, V.R., Syme, G.J. (Eds.), Integrated Assessment of Scale Impacts of Watershed Intervention. Elsevier, pp. 85–98. doi: 10.1016/B978-0-12-800067-0.00004-9.

Ranatunga, K., Nation, E., Barratt, D., 2008. Review of soil water models and their applications in Australia. Environ. Model. Softw. 23, 1182–1206. http://dx.doi.org/10.1016/j.envsoft.2008.02.003.

Rathjens, H., Oppelt, N., Bosch, D.D., Arnold, J.G., Volk, M., 2015. Development of a grid-based version of the SWAT landscape model. Hydrol. Process. 29, 900–914. http://dx.doi.org/10.1002/hyp.10197.

Reddy, V.R., Syme, G.J., 2015. Integrated Assessment of Scale Impacts of Watershed Intervention, Integrated Assessment of Scale Impacts of Watershed Intervention. Elsevier. 10.1016/B978-0-12-800067-0.00013-X.

Ritchie, J.T., 1972. Model for predicting evaporation from a row crop with incomplete cover. Water Resour. Res. 8, 1204–1213. http://dx.doi.org/10.1029/WR008i005p01204.

Sangrey, D., Harrop Williams, K., Klaiber, J., 1984. Predicting ground water response to precipitation. J. Geotech. Eng. 110, 957–975. http://dx.doi.org/10.1061/(ASCE)0733-9410(1984) 110:7(957).

Sharpley, A.N., Williams, J.R., 1990. EPIC-erosion/productivity impact calculator: 1. Model documentation. In: Technical Bulletin-United States Department of Agriculture.

Skaggs, R.W., Youssef, M.A., Chescheir, G.M., 2012. Drainmod: model use, calibration, and validation. Trans. ASABE 55, 1509–1522. http://dx.doi.org/10.13031/2013.42259.

Sloan, P.G., Moore, I.D., 1984. Modeling subsurface stormflow on steeply sloping forested watersheds. Water Resour. Res. 20, 1815–1822. http://dx.doi.org/10.1029/WR020i012p01815.

Steiner, J.L., Sadler, E.J., Wilson, G., Hatfield, J.L., James, D., Vandenberg, B., Chen, J.S., Oster, T., Ross, J.D., Cole, K., 2009. STEWARDS watershed data system: system design and implementation. Trans. ASABE 52, 1523–1533.

Syme, G.J., Reddy, V.R., Pavelic, P., Croke, B., Ranjan, R., 2012. Confronting scale in watershed development in India. Hydrogeol. J. 20, 985–993. http://dx.doi.org/10.1007/s10040-011-0824-0.

Tarboton, D., 2003. Rainfall-Runoff Processes. Utah State Univ., 159.

USEPA (2007). An Approach for Using Load Duration Curves in the Development of TMDLs, EPA 841-B-07-006, August 2007. Watershed Branch (4503T), Office of Wetlands, Oceans and Watersheds, U.S. Environmental Protection Agency, 1200 Pennsylvania Ave. NW. Washington, DC 20460. http://www.epa.gov/OWOW/TMDL/techsupp.html.

Williams, J.R., 1969. Flood Routing With Variable Travel Time or Variable Storage Coefficients. doi: 10.13031/2013.38772.

Williams, J.R., Haan, R.W., 1973. HYMO: Problem oriented language for hydrologic modeling – User's Manual. USDA, ARS-S-9.

Yang, D., Herath, S., Musiake, K., 2000. Comparison of different distributed hydrological models for characterization of catchment spatial variability. Hydrol. Process. 14, 403–416. http://dx.doi.org/10.1002/(SICI)1099-1085(20000228)14:3<403::AID-HYP945>3.0.CO;2-3.

Yang, D., Koike, T., Tanizawa, H., 2004. Application of a distributed hydrological model and weather radar observations for flood management in the upper Tone River of Japan. Hydrol. Process. 18, 3119–3132. http://dx.doi.org/10.1002/hyp.5752.